DRUG MECHANISM

Transcellular stomach absorption of a derivatized glucagon-like peptide-1 receptor agonist

Stephen T. Buckley[1]*†, Tine A. Bækdal[2†], Andreas Vegge[1†], Stine J. Maarbjerg[2], Charles Pyke[1], Jonas Ahnfelt-Rønne[1], Kim G. Madsen[1], Susanne G. Schéele[1], Tomas Alanentalo[1], Rikke K. Kirk[1], Betty L. Pedersen[1], Rikke B. Skyggebjerg[1], Andrew J. Benie[1], Holger M. Strauss[1], Per-Olof Wahlund[1], Simon Bjerregaard[1], Erzsébet Farkas[3], Csaba Fekete[3,4], Flemming L. Søndergaard[2], Jeanett Borregaard[2], Marie-Louise Hartoft-Nielsen[2], Lotte Bjerre Knudsen[1]

Oral administration of therapeutic peptides is hindered by poor absorption across the gastrointestinal barrier and extensive degradation by proteolytic enzymes. Here, we investigated the absorption of orally delivered semaglutide, a glucagon-like peptide-1 analog, coformulated with the absorption enhancer sodium *N*-[8-(2-hydroxybenzoyl) aminocaprylate] (SNAC) in a tablet. In contrast to intestinal absorption usually seen with small molecules, clinical and preclinical dog studies revealed that absorption of semaglutide takes place in the stomach, is confined to an area in close proximity to the tablet surface, and requires coformulation with SNAC. SNAC protects against enzymatic degradation via local buffering actions and only transiently enhances absorption. The mechanism of absorption is shown to be compound specific, transcellular, and without any evidence of effect on tight junctions. These data have implications for understanding how highly efficacious and specific therapeutic peptides could be transformed from injectable to tablet-based oral therapies.

INTRODUCTION

Glucagon-like peptide-1 (GLP-1) is a 30–amino acid incretin peptide hormone, which is secreted by enteroendocrine L cells in the gastrointestinal tract (GIT) and by preproglucagon neurons located in the nucleus of the solitary tract in the hindbrain. Pharmacologically, long-acting GLP-1 receptor agonists (GLP-1RAs) exhibit glucoregulatory functions via a triumvirate of mechanisms, namely, stimulation of insulin release in a glucose-dependent manner, suppression of glucagon activity during hyperglycemia, and a minor delay of gastric emptying resulting in slower glucose absorption (*1*, *2*). In addition, GLP-1 promotes satiety and reduces energy intake by virtue of its neurotransmitter role in brainstem-hypothalamus pathways signaling satiety (*3*, *4*), and some long-acting GLP-1RAs including semaglutide have shown cardiovascular risk reduction (*5*, *6*).

Owing to its rapid degradation by the proteolytic enzyme dipeptidyl peptidase-4 and equally rapid renal clearance, successful application of GLP-1 as a therapy in the treatment of type 2 diabetes (T2D) has necessitated the development of injectable analogs of the native GLP-1 peptide or modified peptides with GLP-1RA properties, which are resistant toward degradation and clearance (*7*). To this end, the incretin mimetic exendin-4 was developed, and subsequently, the first fatty acid–acylated GLP-1RA, liraglutide, providing a once-daily subcutaneously administered analog of human GLP-1. Subsequent optimization of the GLP-1RA class has focused on the ease and frequency of administration, leading to the development of analogs for once-weekly subcutaneous administration such as dulaglutide, an Fc fusion protein. In line with this, recent advancements in fatty acid acylation–based protraction technology have provided the possibility of achieving extended plasma half-lives ($t_{½}$) without increasing molecular size, leading to the discovery of semaglutide, a GLP-1 analog with a $t_{½}$ of ~1 week in humans (*8*). Despite the remarkable pharmacological effects of simultaneous glucose, body weight, and blood pressure lowering and cardiovascular risk reduction already achieved with semaglutide administered subcutaneously, the mode of administration is likely a barrier for some potential users. This barrier could be overcome with the availability of an oral formulation of semaglutide. Conceivably, an orally administered GLP-1RA may lead to earlier initiation of GLP-1RA treatment and improve acceptance and adherence among patients, compared with injectable formulations of GLP-1RAs (*9*).

The inherent physicochemical properties of peptides (high molecular weight, enzymatically labile, hydrophilicity, and low permeability) have hampered attempts to deliver peptides such as GLP-1 via the oral route (*10*). This is mainly because the vast majority of peptides evaluated for oral delivery have been ill-equipped to surmount the challenges presented by the hostile environment of the GIT, which is designed to degrade proteins and peptides ingested in food to di- and tripeptides before absorption in the small intestine. Thus, subtherapeutic exposure and high inter- and intraindividual variability have resulted. In addition, many peptides obtain protraction from the subcutaneous administration site while having a shorter intravenous $t_{½}$, making the duration of action unsuitably short if given orally. Uniquely, fatty acid acylation can achieve $t_{½}$ prolongation independently of the subcutaneous route of administration while having no appreciable impact on the function of the peptide. Collectively, these characteristics make the semaglutide molecule well suited for oral delivery when coformulated with an absorption enhancer, which can sufficiently augment its absorption. Moreover, once-daily administration of a compound with a $t_{½}$ of ~1 week will have a favorable effect on intraindividual variability in exposure. In a phase 2 clinical trial with an oral formulation of semaglutide, a substantial dose-dependent lowering of both glycosylated hemoglobin and body weight was achieved in individuals with T2D (*11*). Currently, oral semaglutide

[1]Novo Nordisk A/S, 2760 Måløv, Denmark. [2]Novo Nordisk A/S, 2860 Søborg, Denmark. [3]Department of Endocrine Neurobiology, Institute of Experimental Medicine, Hungarian Academy of Sciences, 1083 Budapest, Hungary. [4]Department of Medicine, Division of Endocrinology, Diabetes and Metabolism, Tupper Research Institute, Tufts Medical Center, Boston, MA 02111, USA.
*Corresponding author. Email: spby@novonordisk.com
†These authors contributed equally to this work.

is being evaluated in the PIONEER phase 3a clinical trial programme consisting of 10 trials including about 9000 patients with T2D, which will report in 2018.

Here, we report a detailed mechanistic examination into the absorption of semaglutide after oral administration when coformulated with the absorption enhancer, sodium *N*-[8-(2-hydroxybenzoyl) aminocaprylate] (SNAC). These investigations spanned from clinical to basic science research and sequentially unraveled increasing mechanistic details about the absorption of oral semaglutide. Our data establish a unique role for the stomach as an absorptive site for orally delivered peptides coformulated with an absorption enhancer, recommending a judicious approach toward a combination of peptide and absorption enhancer. These findings reconceptualize the previously held tenets of peptide absorption after oral administration and establish a new generalized strategy for successful delivery of therapeutic peptides via the oral route.

RESULTS

Oral semaglutide is absorbed in the stomach

To explore the anatomical site of absorption of oral semaglutide, we performed a series of investigations in humans and in various dog models. Using scintigraphic imaging after single-dose administration of oral semaglutide (10 mg with 300 mg of SNAC; containing ^{111}In-labeled ion-exchange resin) in the fasted state with 240 ml of water, complete tablet erosion (CTE) was observed to occur in the stomach of all evaluable human individuals (mean time to CTE, 57 min). Representative scintigraphic images (Fig. 1A) show that, in this individual, no tablet erosion had occurred 2 min after dosing, whereas no intact tablet core remained after 140 min. Magnetic monitoring studies in dogs, which tracked tablet disintegration, reinforced these observations (fig. S1). Semaglutide plasma concentrations confirmed early systemic absorption and an apparently slow elimination phase once present in the systemic circulation (Fig. 1B). Likewise, SNAC absorption started early and exhibited a fast elimination, with very limited exposure after ~4 to 6 hours (Fig. 1C). Because of the pharmacokinetic implications of once-daily dosing of a compound with a $t_{½}$ of ~1 week, the variability in semaglutide exposure observed after a single dose (Fig. 1B) does not translate into high variability in effect at steady state after 26 weeks of once-daily dosing (as measured by glycosylated hemoglobin; HbA_{1c}) or in unacceptable intolerability in patients with T2D (*11*).

Absorption from the stomach may be hindered by the presence of exogenous effectors such as food. To further substantiate the notion of stomach-based absorption and to clarify the potential impact of the presence of food in the stomach, we carried out a food-effect study in healthy individuals receiving once-daily oral semaglutide in the fed or fasted state for 10 days. Supporting the importance of the stomach as a key absorption site for semaglutide, when dosed in the fed state, no measurable semaglutide exposure was observed in 14 of 25 individuals and limited semaglutide exposure was observed in the remaining 11 individuals on day 10 (Fig. 1D, fed state). In contrast, all individuals dosed in the fasted state had measurable semaglutide exposure (Fig. 1D, fasting state), emphasizing that absorption of oral semaglutide in the stomach is hindered by the presence of food, and thus, administration of oral semaglutide should be in the fasting state. Similar observations were made in analogous studies in dogs, where exposure was shown to decrease with decreasing postdose fasting time (fig. S2).

To support clinical observations of stomach absorption, we performed mechanistic studies in dogs. Prevention of intestinal absorption by pyloric ligation, followed by intragastric semaglutide dosing resulted in semaglutide plasma concentrations comparable to those seen in nonligated dogs receiving oral dosing (Fig. 1E), illustrating that absorption of oral semaglutide can occur in the stomach. To definitively demonstrate the prevailing role of the stomach in the absorption of oral semaglutide, we measured semaglutide plasma concentrations in the splenic vein (vena lienalis; draining the gastric cavity) and in the portal vein (vena porta; draining the gastrointestinal system) after intragastric dosing in nonligated dogs. Concentrations were higher in the splenic vein over the first 30 min after dosing, as reflected by a ratio of the area under the curve ($AUC_{0–30min}$) between the splenic and portal veins of 1.94 [95% confidence interval (CI), 1.15 to 2.74; $P < 0.05$; Fig. 1F], confirming the stomach as the predominant site of absorption. Control studies using paracetamol dosed to the duodenum revealed a ratio of <1, consistent with duodenal absorption (fig. S3). Investigations to evaluate overall plasma exposure levels demonstrated that targeting the stomach achieved a mean bioavailability ± SEM of 1.22 ± 0.25% in the dog model (table S1).

Spatiotemporal factors govern the absorption of oral semaglutide

Efficient absorption of oral semaglutide is dependent on the presence of the absorption enhancer SNAC. We examined the interrelationship between both components, their mutual dependence on the physiological traits of the stomach, and the collective influence of these factors on the extent and nature of the absorption of semaglutide. To establish the concentration of SNAC necessary to confer therapeutically relevant plasma exposure of semaglutide, we administered a single dose of oral semaglutide (5 mg) with either 150 or 300 mg of SNAC to healthy individuals. Semaglutide plasma concentrations were higher when semaglutide was coformulated with 300 mg of SNAC (Fig. 2A), whereas higher amounts (600 mg) led to lower semaglutide plasma concentrations (fig. S4). These results suggest that 300 mg represents an appropriate amount of SNAC to enhance absorption of semaglutide in this formulation, potentially by avoiding salting out effects and precipitation, which may be associated with higher amounts of SNAC. To directly explore the impact of SNAC concentration on its absorption-enhancing actions, we used an in vitro model of the gastric epithelium, NCI-N87. Reflecting the discrete differences in semaglutide plasma exposure observed between 150 and 300 mg of SNAC, moderate concentrations of SNAC were required to adequately enhance the in vitro gastric epithelial permeability of semaglutide. A significant ~7-fold increase in the apparent permeability (P_{app}) of semaglutide was seen with 80 mM SNAC versus control (no SNAC; $P < 0.001$; Fig. 2B).

The concentrations of SNAC and semaglutide at the site of absorption are determined to a great extent by tablet surface erosion kinetics. To investigate the spatiotemporal interplay between concentration and erosion kinetics, we endoscopically aspirated gastric fluid from underneath an oral semaglutide tablet (at 0 cm) and at 3 and 6 cm from the tablet at 15 and 30 min after dosing in anesthetized dogs. Results showed that high concentrations of semaglutide and SNAC were restricted to areas close to the tablet (Fig. 2C). Measured concentrations of semaglutide and SNAC underneath the tablet 30 min after dosing were significantly and >10-fold higher than that measured at 6 cm from the tablet ($P = 0.007$ for semaglutide

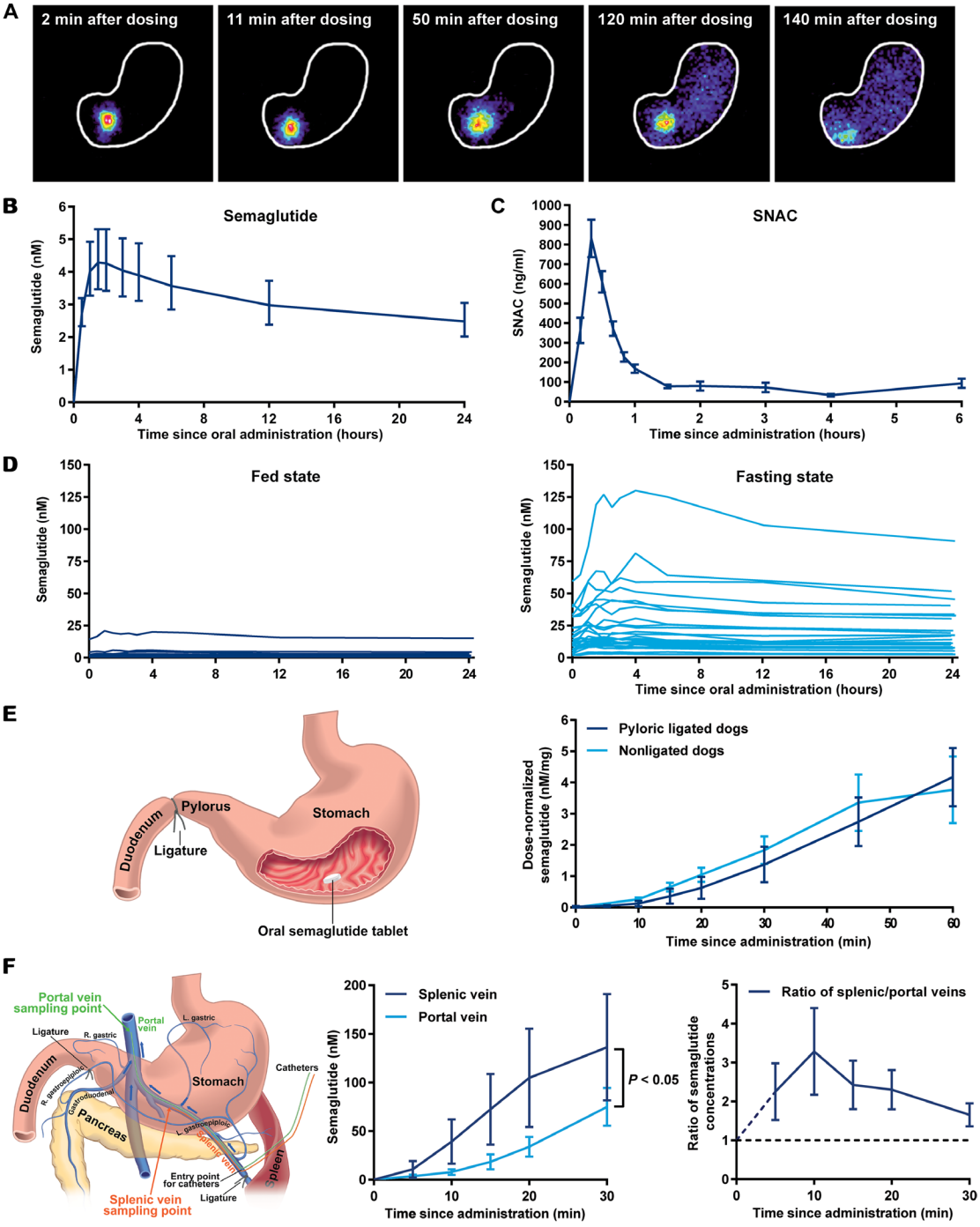

Fig. 1. Anatomical site of absorption of oral semaglutide. (**A**) Gamma scintigraphic imaging of tablet erosion in the stomach from 2 to 140 min after a single dose of oral semaglutide (10 mg) in a representative healthy individual. White line outlines the stomach; colors within the stomach (red/yellow/green/blue) represent the tablet core and released radioactivity. (**B**) Estimated mean semaglutide plasma concentration–time profile after a single dose of oral semaglutide (10 mg) in healthy individuals ($n = 26$). (**C**) Arithmetic mean SNAC plasma concentration–time profile after a single dose of oral semaglutide (10 mg) in healthy individuals ($n = 26$). (**D**) Individual semaglutide plasma concentration–time profiles on day 10 of once-daily dosing of oral semaglutide in fed ($n = 25$) and fasting ($n = 26$) states, respectively, in healthy individuals. (**E**) An illustration of pyloric ligation, which prevents intestinal absorption, and mean dose-normalized semaglutide plasma concentration–time profiles after a single dose of oral semaglutide (9.4 to 12.7 mg) in pyloric ligated ($n = 6$) and nonligated ($n = 16$) beagle dogs. (**F**) Illustration of the splenic vein, which drains the gastric cavity, and the portal vein, which drains the gastrointestinal system. Mean semaglutide plasma concentration–time profiles in the splenic and portal veins after a single dose of oral semaglutide (10 mg) in beagle dogs ($n = 15$). R. gastric, right gastric; L. gastric, left gastric; R. gastroepiploic, right gastroepiploic; L. gastroepiploic, left gastroepiploic. The ratio and 95% CI of the splenic versus portal veins for $AUC_{0–30min}$ were calculated [1.94 (1.15 to 2.74)], and statistical significance was determined on the basis of a null hypothesis value of 1 ($P < 0.05$). The horizontal dashed line (right) represents similar semaglutide plasma concentrations in the splenic and portal veins. Error bars show ±SEM calculated on the original scale (C, E, and F) or calculated on a log-scale and back-transformed to the original scale (B).

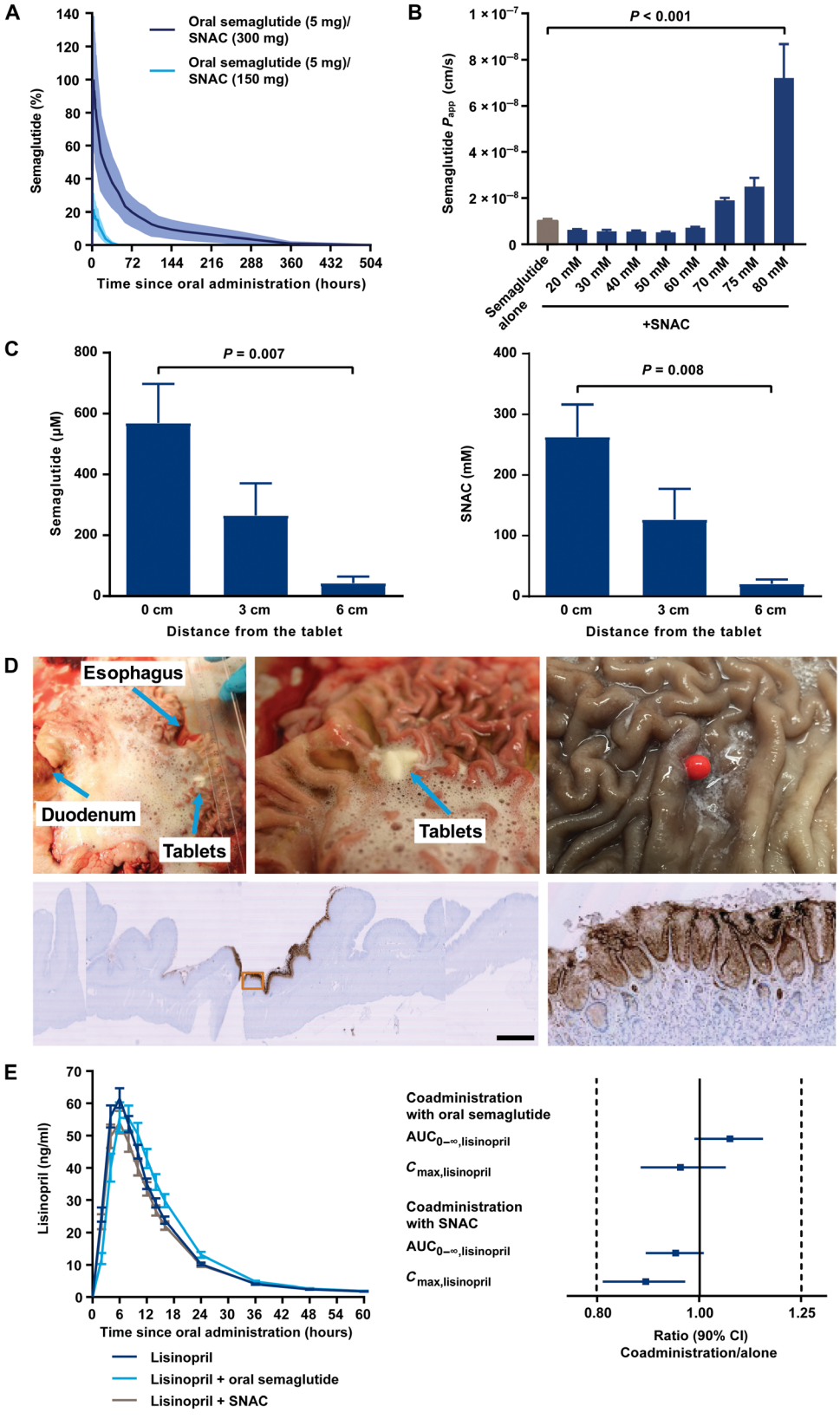

Fig. 2. Localized absorption of oral semaglutide in gastric mucosa close to the tablet. (**A**) Arithmetic mean semaglutide plasma concentration–time profiles after a single dose of oral semaglutide (5 mg) with varying amounts of SNAC in healthy males (n = 10 per treatment arm). Semaglutide plasma concentrations are expressed as the percentage of the maximum mean concentration for oral semaglutide (5 mg)/SNAC (300 mg). For individuals with no measurable semaglutide plasma concentration, concentrations were set to zero. (**B**) Mean P_{app} of semaglutide across monolayers of NCI-N87 cell cultures in the absence and presence of SNAC. n = 14 (semaglutide alone), n = 4 (20 to 75 mM SNAC), or n = 17 (80 mM SNAC). P_{app} was greater for 80 mM SNAC versus semaglutide alone (P < 0.001) as tested by a two-tailed Student's t test. (**C**) Mean concentrations of semaglutide and SNAC in gastric fluid aspirated from underneath an oral semaglutide tablet (at 0 cm) and at 3 and 6 cm from the tablet 30 min after dosing in beagle dogs (n = 8). Concentrations of semaglutide and SNAC were higher underneath the tablet than at 6 cm from the tablet (P = 0.007 for semaglutide and P = 0.008 for SNAC) as tested in one-way analysis of variances (ANOVAs) with multiple comparisons. (**D**) Gross and histological images of tissue from beagle dogs after oral semaglutide dosing. Red pin in gross image (top row, right) corresponds with localization of tablet remnants. Immunoreactivity of semaglutide is shown in brown (bottom row). (**E**) Geometric mean lisinopril plasma concentration–time profiles after administration of lisinopril alone (n = 52) and after coadministration with oral semaglutide (n = 46) or SNAC (n = 50) in healthy individuals and estimated ratios between coadministration and administration alone for $AUC_{0-\infty,lisinopril}$ and $C_{max,lisinopril}$ from ANOVA models with the log-transformed end point as dependent variable and participant and treatment as fixed effects. There were no effects of oral semaglutide or SNAC coadministration because the 90% CIs for the ratios of coadministration/alone were within the predefined interval of 0.80 to 1.25. Error bands show ±SEM (A). Error bars show SEM (B and C) and ±SEM calculated on a log-scale and back-transformed to the original scale (E, left) or 90% CI (E, right).

and $P = 0.008$ for SNAC). Further corroborating the localized nature of semaglutide absorption, the immunoreactivity of semaglutide in stomach tissue was restricted to epithelial surfaces immediately under and around the site of tablet identification (Fig. 2D).

To clarify the importance of spatial proximity on the absorption-enhancing actions of SNAC, we investigated the impact of concomitant administration of oral semaglutide with lisinopril, a Biopharmaceutics Classification System III compound (poorly permeable, highly soluble), on the pharmacokinetics of lisinopril in humans. Coadministration of lisinopril with either SNAC alone or oral semaglutide did not influence lisinopril plasma concentrations, as reflected by unchanged $AUC_{0-\infty,lisinopril}$ and maximum concentration ($C_{max,lisinopril}$; Fig. 2E). Thus, the coformulation, rather than just coadministration, of SNAC with semaglutide is necessary for achieving efficient absorption enhancement.

Absorption efficacy depends on the coformulation of GLP-1 analog and absorption enhancer

Efficient absorption is contingent on suitable interplay between the absorption enhancer and its coformulated peptide. To investigate this, we evaluated the plasma exposure of semaglutide and liraglutide, another structurally distinct analog of GLP-1, after oral dosing with SNAC in rats. $AUC_{0-180min}$ was significantly lower for liraglutide compared to semaglutide ($P = 0.002$; Fig. 3A). The SNAC orthoisomer, *o*-SNAC, showed a markedly diminished absorption-enhancing effect compared to SNAC (Fig. 3, B and C, and fig. S5).

SNAC engages with cell membranes to promote transient enhanced absorption of semaglutide

To explore how SNAC promotes absorption, we examined the intracellular accumulation of semaglutide during passage across NCI-N87 monolayers after exposure to SNAC or EDTA, a modulator of tight junction function (*12*), and subsequent addition of semaglutide. Exposure to SNAC substantially increased the intracellular accumulation of semaglutide compared to control cells ($P < 0.001$; Fig. 3D). In contrast, EDTA had no significant effect compared to control ($P = 0.057$) despite enhancing the P_{app} of semaglutide to a similar magnitude as SNAC (Fig. 3E).

The duration of the transcellular enhancing action of SNAC will, to a considerable extent, define its functional performance. To provide a deeper understanding of the duration of action of SNAC, we examined the barrier properties of segments of rat gastric mucosa mounted in Ussing chambers upon exposure to SNAC. A 25% decline ($P = 0.048$) in TEER was recorded after a time-limited exposure to SNAC, which was restored within 60 min ($P = 0.286$; Fig. 3F). Histological samples taken 30 and 120 min after exposure to SNAC displayed an intact gastric mucosa populated with flattened to cuboidal epithelium (Fig. 3G) and mirrored observations after exposure to ethanol or acetylsalicylic acid (fig. S6). Emphasizing its relatively short duration of action, the increased P_{app} of semaglutide elicited by SNAC at 10 min compared to baseline ($P = 0.008$) gradually declined toward the baseline at 30 min after exposure ($P = 0.142$) and 60 min after exposure ($P = 0.568$) after the removal of SNAC (Fig. 3H). In addition, the enhancing actions of SNAC were observed to be size dependent, with a diminishing effect on the transport of molecules as they exceed 4 kDa (fig. S7).

A transcellular mechanism of action requires the interaction of SNAC with lipid membranes. Physical interactions between SNAC and lipid membranes were characterized by high-sensitivity differential scanning calorimetry. Using DMPC membranes, increasing concentrations of SNAC yielded a gradual reduction in the main transition temperature (T_m), indicating that SNAC is incorporated in and fluidizes the lipid membrane (Fig. 3I). To confirm whether these interactions correspond to changes in membrane permeability, we examined leakage of an encapsulated marker CF from EPC/cholesterol liposomes upon exposure to SNAC. Increasing millimolar concentrations of SNAC increased release of CF, whereas no appreciable effect was observed in the presence of sodium salicylate despite its structural similarities (Fig. 3J and fig. S8).

SNAC promotes monomerization of semaglutide

Fatty acid–acylated GLP-1 analogs are known to form oligomers (*13*), which could affect absorption. We examined the effect of SNAC on semaglutide self-association using three orthogonal biophysical characterization techniques: NMR spectroscopy, DLS, and analytical ultracentrifugation. Increasing the concentration of SNAC at a constant concentration of semaglutide resulted in a decrease in the apparent molecular mass, which is consistent with a shift in the oligomeric state of semaglutide toward its monomeric form (Fig. 3, K and L). This effect was not simply due to increased ionic strength of the system because the addition of 120 mM sodium chloride did not induce a similar monomerization (fig. S9).

SNAC exerts buffering actions in the gastrointestinal milieu to attenuate enzymatic activity

To examine the behavior of SNAC in the stomach, we incubated oral semaglutide tablets containing SNAC in small volumes (1 to 30 ml) of SGF and monitored the pH of the dissolution media as the tablets dissolved. SNAC augmented the pH of SGF from acidic to neutral within 5 to 15 min (Fig. 3M). The buffering effect of SNAC was inversely related to the volume (1 ml > 3 ml > 10 ml > 30 ml) and the type of SGF used (more efficient in diluted SGF), whereas a semaglutide tablet without SNAC had no apparent effect on pH (fig. S10).

The primary digestive enzyme in the stomach is pepsin. Optimal pepsin activity is observed at low pH, such as that found in gastric fluid of the stomach (pH 2 to 4) (*14*). Given the peptide character of semaglutide, it is reasonable to expect that pepsin may degrade semaglutide in the stomach. However, in light of the pronounced buffering effect of SNAC, the impact of pH on semaglutide stability was examined in the presence of pepsin. Semaglutide was incubated with pepsin (3.5 U/ml) at pH values of 2.6, 5.0, and 7.4, and the $t_{½}$ was calculated, assuming first-order degradation kinetics. In agreement with the pH-dependent activity of pepsin, the effect of pepsin on semaglutide stability was most profound at low pH, with semaglutide being most labile toward pepsin at pH 2.6 ($t_{½}$ = 16 min; Fig. 3N). In contrast, increasing the pH to 5.0 extended the $t_{½}$ of semaglutide to 34 min, and at neutral pH, semaglutide was almost entirely stabilized ($t_{½}$ > 100 min; Fig. 3N). Although a similar pattern was observed for native GLP-1, its overall stability toward enzymatic degradation was substantially less than that shown for semaglutide (fig. S11).

Semaglutide localizes predominantly to the surface mucous pit regions of the gastric epithelium

To provide a deeper insight into the behavior of semaglutide at the absorptive site in the stomach, we used immunofluorescence imaging on canine gastric tissue. After dosing, intense immunoreactivity for semaglutide was confined to the region in and around the site of tablet identification, whereas semaglutide staining was conspicuous

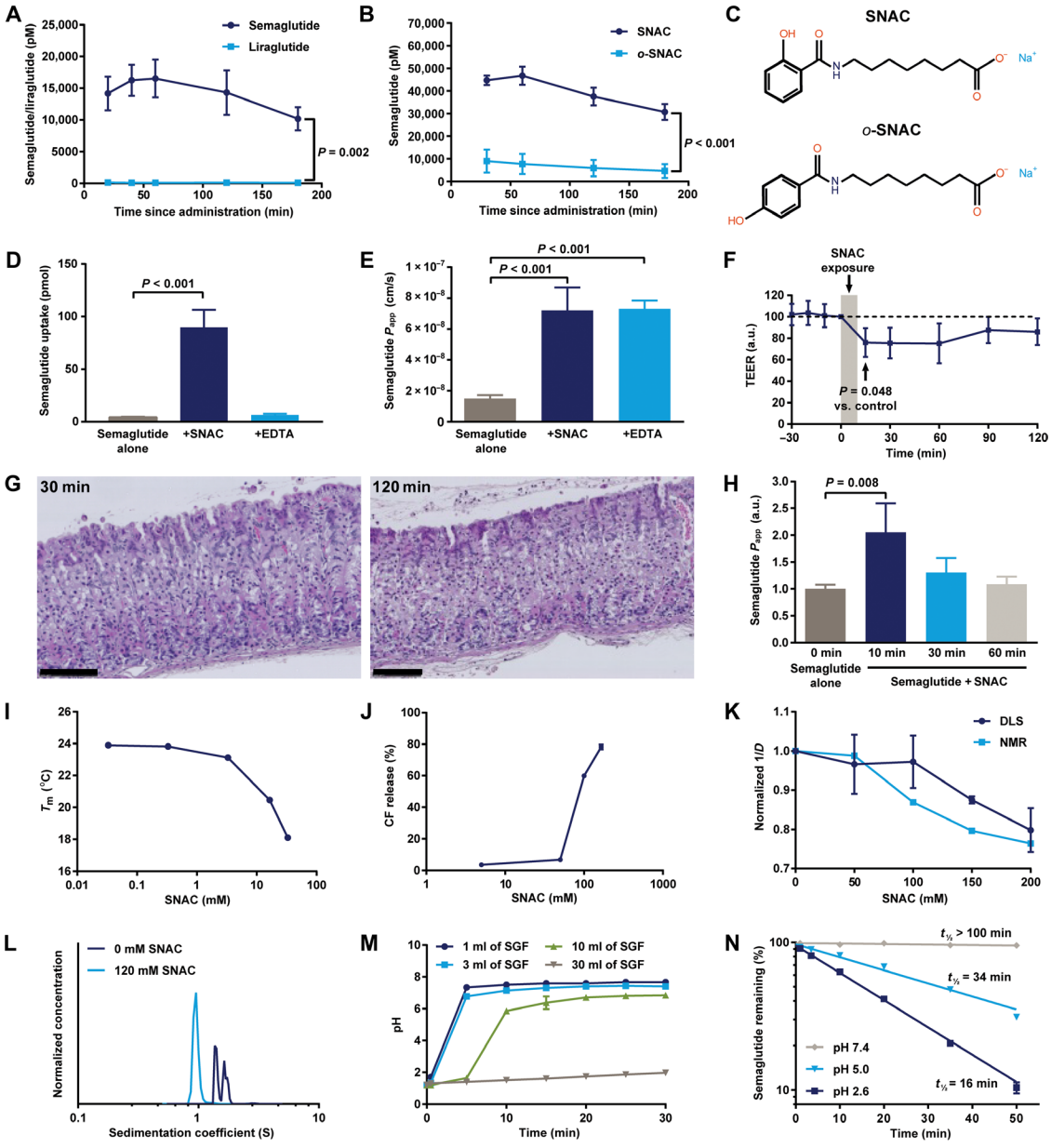

Fig. 3. Mechanisms via which SNAC enhances semaglutide absorption. (**A**) Arithmetic mean semaglutide and liraglutide plasma concentration–time profiles after oral dosing with SNAC in Sprague-Dawley rats ($n = 3$ for semaglutide and $n = 4$ for liraglutide). $AUC_{0–180min}$ was greater for semaglutide versus liraglutide ($P = 0.002$) as tested by a two-tailed Student's t test. (**B**) Arithmetic mean semaglutide plasma concentration–time profiles after oral dosing with SNAC or o-SNAC in Sprague-Dawley rats ($n = 6$ for SNAC and $n = 8$ for o-SNAC). $AUC_{0–180min}$ was greater with SNAC versus o-SNAC ($P < 0.001$) as tested by a two-tailed Student's t test. (**C**) Chemical structures of SNAC and o-SNAC. (**D**) Intracellular uptake of semaglutide in monolayers of NCI-N87 cell cultures after exposure to semaglutide alone, semaglutide + SNAC (80 mM), or semaglutide + EDTA (75 mM; $n = 8$ per treatment group). Semaglutide uptake was greater for semaglutide + SNAC versus semaglutide alone ($P < 0.001$) as tested by a two-tailed Student's t test. (**E**) P_{app} of semaglutide across monolayers of NCI-N87 cell cultures after exposure to semaglutide alone ($n = 18$), semaglutide + SNAC (80 mM; $n = 17$), or semaglutide + EDTA (75 mM; $n = 4$). Semaglutide P_{app} was greater for semaglutide + SNAC and semaglutide + EDTA versus semaglutide alone ($P < 0.001$) as tested by two-tailed Student's t tests. Data for semaglutide alone and semaglutide + SNAC are repeated in fig. S5 as comparators. (**F**) Transepithelial electrical resistance (TEER) in rat gastric mucosa after exposure to SNAC (30 mM) for 10 min ($n = 6$). At 15 min, TEER was lower for SNAC-exposed tissue versus control ($P = 0.048$) as analyzed in a Kolmogorov-Smirnov test comparing TEER values of the control and SNAC-exposed tissue at each time point. (**G**) Hemotoxylin and eosin staining of rat gastric mucosa 30 and 120 min after exposure to SNAC. Scale bars, 100 μm. (**H**) P_{app} of semaglutide after exposure of rat gastric mucosa to semaglutide alone ($n = 18$) or to SNAC from 0 to 10 min with subsequent addition of semaglutide at 10 min ($n = 8$), 30 min ($n = 5$), or 60 min ($n = 7$). Semaglutide P_{app} was greater when semaglutide was added after 10 min of SNAC exposure versus semaglutide alone ($P = 0.008$) as tested by a two-tailed Student's t test. (**I**) Change in main transition temperature (T_m) of dimyristoylphosphatidylcholine (DMPC) membranes upon exposure to increasing concentrations of SNAC. The plotted T_m values were determined from individual thermograms generated for each concentration. (**J**) Release of carboxyfluorescein (CF) from egg phosphatidylcholine (EPC)/cholesterol liposomes after incubation with increasing concentrations of SNAC ($n = 3$). (**K**) Normalized $1/D$ as measured by nuclear magnetic resonance (NMR) and dynamic light scattering (DLS) upon exposure of semaglutide to increasing concentrations of SNAC [$n = 1$ for NMR, $n = 3$ for DLS (0 to 150 mM SNAC), and $n = 2$ for DLS (200 mM SNAC)]. (**L**) Sedimentation coefficient distributions measured by analytical ultracentrifugation in the absence and presence of SNAC ($n = 1$). Data for the 0 mM SNAC condition are repeated in fig. S9 as comparator. (**M**) pH during 30-min incubation of semaglutide + SNAC tablets in different volumes of simulated human gastric fluid (SGF; $n = 3$ per group). (**N**) Percentage remaining of intact semaglutide and calculated $t_{½}$ upon incubation with pepsin (3.5 U/ml; $n = 4$ per group). Error bars show ±SEM (A, B, F, J, K, M, and N) or SEM (D, E, and H). a.u., arbitrary units.

by its absence in regions remote to the tablet surface (Fig. 4A). Together, these data further substantiate the suggestion that absorption occurs in a highly localized environment in the stomach. Closer examination of semaglutide localization revealed that reactivity was mostly restricted to the surface mucous epithelial cell layer in the pit and neck regions of the gastric mucosa (Fig. 4B), which was also confirmed in rats via light microscopy (fig. S12). In contrast, the bulk of gastric hydrogen potassium ATPase (H^+/K^+ ATPase)–positive parietal cells were observed within deeper layers, although a few scattered parietal cells were found in the neck region. Sloughing of surface mucous epithelial cells containing semaglutide immunoreactivity was evident in discrete regions, but the most abundant immunohistochemical signal for semaglutide was detected in deeper, intact layers where robust expression of ZO-1, a tight junction protein, was detected at the apical surface (Fig. 4, C and D). Intracellular uptake of semaglutide was revealed by cytoplasmic immunoreactivity in mucosal epithelial cells of the stomach (Fig. 4E). Semaglutide was detected within blood vessels of the lamina propria mucosae 5 min after dosing (Fig. 4F and movie S1) and in the systemic circulation 5 min after dosing (~1000 to 2000 pM), emphasizing its apparent early uptake.

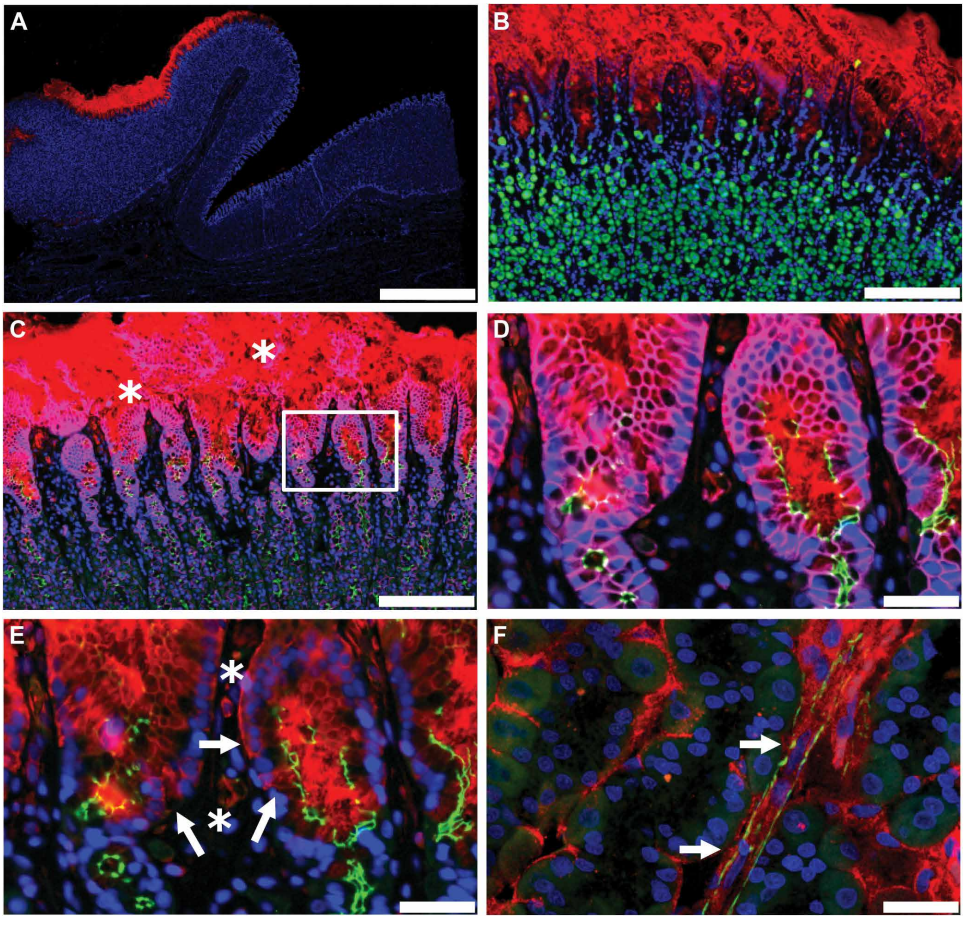

Fig. 4. Absorption and localization of semaglutide in dog gastric mucosa. (**A**) Local 3F15 (semaglutide) immunofluorescence reactivity (red) under the tablet. Nuclei counterstained with 4′,6-diamidino-2-phenylindole (DAPI; blue). Scale bar, 2 mm. (**B**) 3F15 reactivity (red) restricted to the neck region. The bulk of H^+/K^+ ATPase (green)–positive parietal cells reside in deeper layers, but a few scattered parietal cells can be found in the neck region exposed to luminal semaglutide. Scale bar, 200 μm. (**C**) 3F15 (red), β-catenin (purple), ZO1 (green), and DAPI (blue). Sloughing of the uppermost region of the epithelium is marked by white asterisks; semaglutide is also detected in deeper, intact layers (white box). Scale bar, 200 μm. (**D**) Higher magnification of the boxed area in (C). Intact tight junctions labeled with apical ZO1 (green) in direct contact with luminal semaglutide. Scale bar, 40 μm. (**E**) Same region as (D) without β-catenin. Intracellular 3F15 reactivity (red) is observed in mucosal cells (marked by white arrows). 3F15 also detects semaglutide in capillaries under the epithelium (marked by white asterisks). Scale bar, 40 μm. (**F**) Maximum projection image from a 63× confocal 11-μm *z* stack, showing semaglutide (red) associated with a blood vessel (marked by white arrows) labeled with smooth muscle actin (green). Scale bar, 40 μm.

Semaglutide concentrates within surface mucous cells

Electron microscopy (EM) studies on gastric mucosa from rats after dosing with oral semaglutide showed signal for semaglutide in the superficial and neck zones of the mucosa, most apparent in the superficial layer of the mucosa by intense labeling in surface mucous epithelial cells (Fig. 5, A and B). In these cells, robust immunoreactivity was observed in the cytoplasm among the mucous vesicles, although the mucous vesicles themselves remained unlabeled (Fig. 5A). Immunoreactivity was also apparent in the basal cytoplasm of the mucous cells (Fig. 5B), indicating transcellular transport of semaglutide. Junctional complexes were intact between the apical portions of mucous-secreting cells, underscoring the absence of paracellular-directed absorption (Fig. 5C). Immunoreactivity was not present in the extracellular space among the mucous cells under junctional complexes, further substantiating a transcellular mode of absorption. In the neck region of the gastric glands, silver grains were observed in the cytoplasm and on the microvilli of the intracellular canaliculi of parietal cells (Fig. 5D).

Luminal semaglutide does not interact with GLP-1Rs on parietal cells in the corpus mucosa

To evaluate the distribution of GLP-1Rs in gastric epithelium, we performed double in situ hybridization (ISH)/immunohistochemistry (IHC) for GLP-1R and H^+/K^+ ATPase on sections from rat stomach and ISH for GLP-1R alone in human stomach sections. GLP-1Rs were expressed on virtually all H^+/K^+ ATPase–positive parietal cells of the gastric pits in rat (Fig. 6, A to C), and a similar distribution was also observed in human specimens (Fig. 6D). GLP-1R immunoreactivity was absent from the apical surface of the gastric epithelium, thus precluding any direct interactions between luminal semaglutide and GLP-1Rs. Although GLP-1 is reported to have an inhibitory effect on acid secretion (*15*), data from human individuals dosed with oral semaglutide (10 mg) for 10 days revealed no functionally appreciable change in

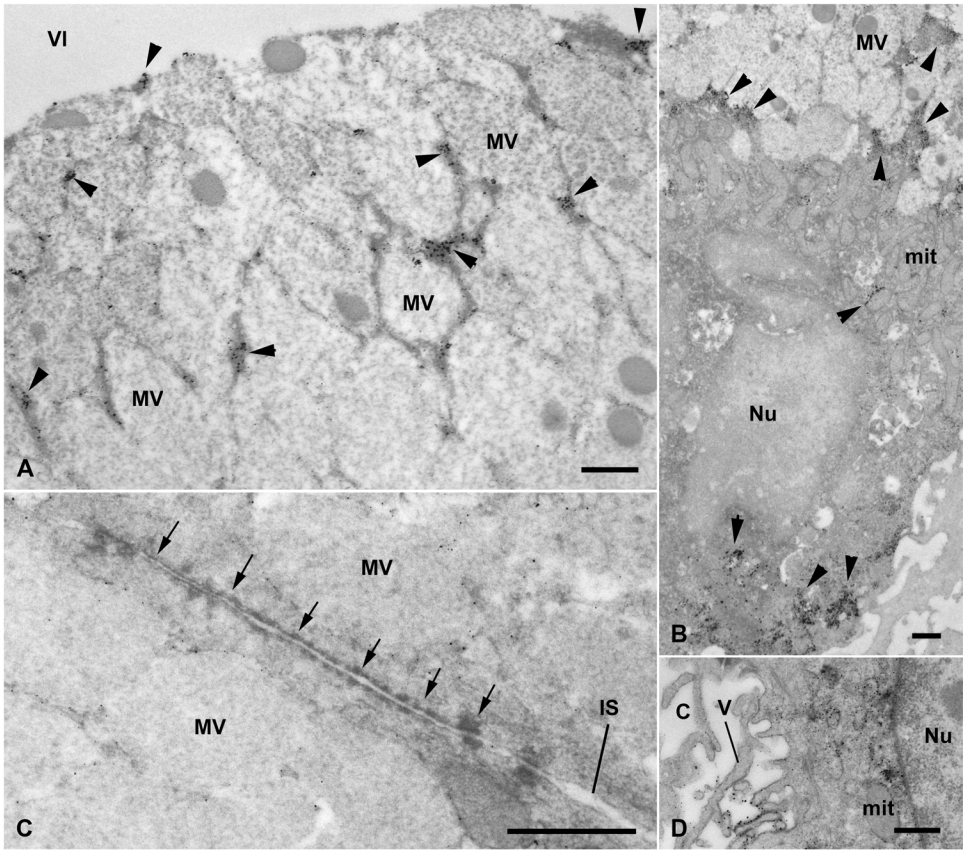

Fig. 5. Ultrastructural examination of the localization of semaglutide in rat gastric mucosa. (**A** and **B**) Transmission EM images of semaglutide immunoreactivity (silver grains, denoted by arrowheads) present in the cytoplasm of mucous cells among the mucous vesicles and also in the basal part (B) of the mucous cells. Silver grains are not present in the mucous vesicles. (**C**) Junctional connection/complexes between the apical parts of the mucous cells (indicated by the arrows). Silver grains are absent from the intercellular space under the junctional complexes. (**D**) Semaglutide immunoreactivity in parietal cells. Silver grains are observed in the cytoplasm of the parietal cells and on the microvilli of the intracellular canaliculi of these cells. Scale bars, 500 nm. C, intracellular canaliculi; IS, intercellular space; mit, mitochondria; MV, mucous vesicles; Nu, nucleus; V, microvilli; Vl, ventricular lumen.

gastric pH between baseline [3-hour average pH (95% CI), 2.04 (1.83 to 2.28)] and day 9 [2.29 (2.04 to 2.56); $P = 0.154$; Fig. 6E], thereby underscoring the absence of luminal engagement between semaglutide and GLP-1Rs.

DISCUSSION

Here, we report mechanistic investigations into the absorption of orally administered semaglutide, a fatty diacid–acylated GLP-1RA with an extended $t_{½}$, when coformulated in tablets with SNAC, a small fatty acid derivative. This coformulation provides unique, site-directed release and absorption in the stomach and effectively surmounts inherent challenges relating to solubility, molecular size, and proteolytic lability to achieve therapeutically relevant plasma exposure of semaglutide (fig. S13).

Conventionally, the small intestine is considered the major site of drug absorption in the GIT. This is primarily due to its absorptive epithelium and large surface area, which is attributable to the microvillus structure of the epithelial mucosae (*16*). In contrast, a role for the stomach as an absorptive organ for peptides and proteins has been almost entirely disregarded (*17*). Although this understanding of oral drug disposition holds true for small molecules, which are seldom prone to enzymatic degradation and do not require coformulation with absorption-enhancing excipients, our data indicate that the stomach represents an especially apt region of the GIT for absorption of peptide drugs such as semaglutide when coformulated with an absorption enhancer. Pharmacoscintigraphic imaging in humans illustrated that SNAC-containing semaglutide tablets undergo surface erosion in the stomach, followed by an early absorption of semaglutide. Owing to the inherent susceptibility of peptides to enzymatic degradation, it is anticipated that achieving intact semaglutide in the systemic circulation most likely requires absorption very close to the site of disintegration of the semaglutide-containing tablet. Supporting this, mechanistic studies illustrated that exposure in dogs that underwent pyloric ligation reached amounts comparable to that in nonligated dogs and that concentrations measured in plasma from the splenic vein were higher than that from the portal vein. In addition, IHC revealed semaglutide staining in the stomach mucosa only directly under and in close vicinity of the tablet. These data demonstrate that absorption takes place in the environs of the stomach, redefining our previous understanding of absorption of peptides after oral administration. Although the eventuality of a tablet reaching the intestine cannot be unconditionally excluded, the results from the scintigraphy trial showed that 100% of participants had CTE in the stomach, which suggests that the risk of the tablet leaving the stomach is low. Given the protease-rich environment of the small intestine and dilution of both SNAC and semaglutide, the likelihood of absorption from the small intestine is low(er). However, by dosing a compound with a long $t_{½}$ such as semaglutide once daily, the impact of reduced absorption on single days will have minimum impact on the overall steady-state exposure.

Toward elucidating the mechanism of absorption of oral semaglutide, in vitro studies revealed that adequately high concentrations of SNAC are necessary to elicit its absorption-enhancing and buffering effects. Dilution in the GIT is an obstacle for absorption of orally delivered peptides and is a likely contributor to the high variability previously reported in many clinical trials (*18*). This is supported by earlier investigations with an orally delivered calcitonin where increasing volumes of coadministered water (*19*) and food intake (*20*) led to significant reductions in bioavailability. We saw marked differences in semaglutide plasma exposure when humans were dosed with 150 compared to 300 mg of SNAC. Moreover, postprandial administration of semaglutide to individuals resulted in an almost complete

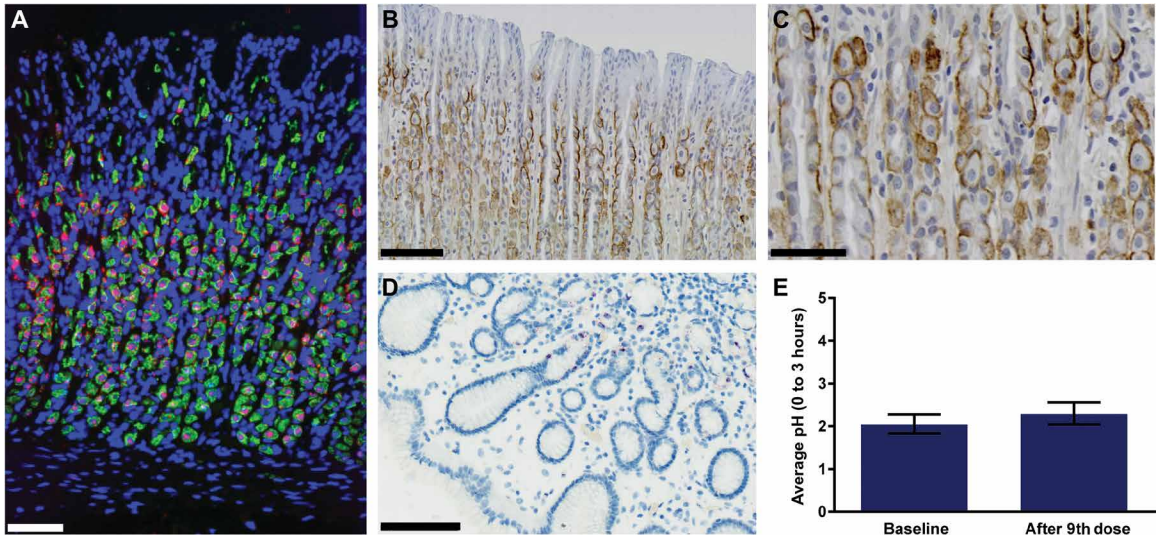

Fig. 6. GLP-1R expression in rat and human gastric mucosa and gastric pH in human individuals. (**A**) GLP-1R mRNA (red signal, RNAscope ISH) in parietal cells (green signal, IHC for ATPase, a marker of parietal cells) in rat corpus mucosa. Scale bar, 50 μm. (**B** and **C**) GLP-1R (brown) membrane-associated staining of parietal cells in corpus mucosa. Scale bars, 100 and 50 μm (B and C, respectively). (**D**) GLP-1R mRNA (blue) in human stomach. Scale bar, 100 μm. (**E**) Average pH over 3 hours at baseline and after the ninth dose of oral semaglutide in healthy individuals ($n = 28$). There was no difference in gastric pH between baseline and day 9 as analyzed in an ANOVA model with logarithmic transformed 3-hour average pH as dependent variable and participant and day (baseline or day 9) as fixed effects. Error bars show the 95% CI.

abolition of semaglutide absorption. Conceivably, food and/or liquid could result in greater dilution of SNAC and semaglutide and thereby curtail the establishment of a concentration gradient sufficient to permit enhanced absorption. To minimize the impact of dilution effects, our investigations indicate that targeted delivery to and subsequent absorption in the stomach is an effective strategy, which is sufficient for achieving the desired pharmacological effect of semaglutide (*11*), albeit with a magnitude of absorption that remains limited compared to that typically achieved with small molecules. The inherent properties and behavior of the small intestine (rapid intestinal transit rate, spreading, and dilution) can substantially curb the absorption of orally administered peptides. This precludes the likelihood of local exposure of the intestinal epithelium to sufficiently high concentrations of absorption enhancer and peptide for an adequately long period of time to permit efficient absorption. Although dispersion processes in the small intestine remain relatively poorly understood, investigations by Lee *et al.* (*21*) revealed that delivery of calcitonin to the lower segment of the small intestine was preferable compared to the upper segment where dilution and spreading effects were particularly marked. Movements through the duodenum are fast, as reflected by a mean contraction frequency of 10 min^{-1}, whereas in the stomach, it is substantially less (3 min^{-1}) (*22*). This is in line with the dominant gastric contraction frequency of 5 to 6 min^{-1} observed using magnetic monitoring in dogs, when the magnetic tablet is disintegrating in the stomach. Previous efforts to surmount the inherent challenges of the small intestine have focused on mucoadhesive approaches, which provide for a privileged region to overcome dilution effects (*23*). Our data indicate that the stomach may provide an environment that permits close contact between the tablet surface and the gastric wall and thereby minimizes spreading and dilution effects. This ensures that local concentrated release of both semaglutide and SNAC is achieved, as reflected by the pronounced concentration gradients measured in gastric fluids in and immediately around the tablet. Semaglutide immunoreactivity was similarly confined to the region of mucosa underneath the tablet, thereby emphasizing the local nature of the absorption process. Absorption kinetics and bioavailability of lisinopril remained unchanged when dosed simultaneously with either oral semaglutide or SNAC alone, which is consistent with previous reports (*24*, *25*). Evidently, close spatial proximity is crucial to ensuring a stable and concentrated exposure of the epithelium to both components. This is only achieved via coformulation, which ensures contemporaneous corelease of both the absorption enhancer (SNAC) and peptide (semaglutide) and in turn nullifies the likelihood of any effects on coadministered drugs.

Although the low pH environment of the stomach could conceivably compromise the solubility of SNAC and semaglutide, our investigations revealed that SNAC neutralizes the microenvironment surrounding the tablet as it undergoes surface erosion and, in doing so, effectively obviates any impact of an unfavorably low stomach pH. The two pK_a values (the logarithmic acid dissociation constant) of SNAC ($pK_a^1 = 4.5$; $pK_a^2 = 8.6$) confer a local buffering capacity, whereby in its deprotonated form, SNAC can neutralize the acidic pH of the stomach. This localized buffering action of SNAC is beneficial with respect to its capacity to stabilize semaglutide upon exposure to gastric fluids while also ensuring sufficient solubility of both components. As a peptide, semaglutide is proteolytically labile and rapidly degraded in the harsh environment of the GIT. Cleavage of peptide bonds commences in the stomach and is driven by pepsin, an aspartate protease, and subsequently by the serine proteases, chymotrypsin and trypsin, in the small intestine (*26*). Their activity is regulated by pH. Although previous attempts have been made to curtail enzymatic degradation via modulation of pH, these efforts have been restricted to the small intestine where acid-based excipients have been used to depress the local pH and thereby attenuate serine protease activity (*27*). Here, we report the effective use of pH modulation in the stomach, where the buffering actions of SNAC facilitate a high local pH and thereby confer enhanced protection of semaglutide from degradation by gastric enzymes, whose

action is most predominant at low pH, and improved solubility of semaglutide.

Although previous reports suggest that SNAC forms weak, noncovalent complexes with peptides and thereby facilitates its enhanced absorption (*28*), our biophysical investigations do not support direct interactions between SNAC and semaglutide. Instead, SNAC indirectly weakens self-association interactions to monomerize semaglutide. Because of its amphiphilic nature, semaglutide forms assemblies that are held together by noncovalent interactions (oligomers). At millimolar concentrations in the stomach, most of semaglutide will be present as oligomers. SNAC triggers changes in the polarity of the solution in which tablet dissolution ensues, which weakens the hydrophobic interactions necessary for oligomerization. SNAC does not form micelles, nor is it positively adsorbed at interfaces. Consequently, it cannot be regarded as a classical surfactant (*29*). Nevertheless, SNAC is capable of partitioning into membranes and affecting their physicochemical properties. Owing to its lipophilic character, SNAC efficiently inserts into the plasma membrane of the gastric epithelium, thereby modifying the inherent packing integrity of cholesterol, phospholipids, and proteins, which in turn affects membrane fluidity (*30*). A delicate balance exists between the necessities for SNAC and semaglutide to exist in both their uncharged form (for insertion into and traversing across the membrane, respectively) and charged form (to achieve high concentrations at the membrane due to higher solubility). Uniquely, the stomach offers an environment where these two opposing needs can be effectively accommodated, whereas in regions of the GIT distal to the stomach, the presence of transiently high concentrations of the uncharged species would be effectively precluded by virtue of the universally higher pH environment. Consistent with its membrane-directed actions, SNAC augmented the cellular uptake of semaglutide in gastric epithelial cells, whereas an exclusively paracellular enhancer (EDTA) had no appreciable effect. Previous studies have shown that membrane interactions have a conspicuous impact on the transepithelial passage of fatty acid–acylated peptides (*31*). Trier *et al.* (*31*) suggest that the optimal fatty acid acylation is a subtle balance between achieving optimal membrane interactions and concurrently avoiding that the degree of membrane insertion becomes excessive so as to hinder translocation. GLP-2 analogs favored short- and medium-length acylations (*31*). For semaglutide, its diacid moiety affords a suitable counterbalance to the membrane-binding properties conferred by a C18 acyl chain. Moreover, use of a transcellular absorption enhancer such as SNAC favorably alters the dynamics and strength of semaglutide's membrane insertion because of its membrane fluidizing effect. Combined, this provides an optimal balance for ensuring efficient membrane insertion and subsequent permeation. Subtle differences in chemical structure can significantly affect these parameters. Modifying the position of the hydroxyl group in SNAC (*o*-SNAC) hinders its propensity to insert into cellular membranes by changing fatty acid orientation and electron distribution in the benzene ring. For liraglutide, its linker-free C16 monoacid acylation imparts keener membrane-binding properties relative to semaglutide, which hinders its efficient transcellular passage, while its proneness to form sizeable heptameric oligomers (*13*) makes it less amenable to the monomerizing actions of SNAC. Together with these observations revealing a blunted absorption upon exchange of peptide or absorption enhancer with a chemically distinct but related analog, we demonstrate the existence of interdependency between peptide and absorption enhancer, which necessitates a tailored and attuned approach to the selection of each respective constituent and disfavors simple indiscriminate combinations. Potentially, this may account for why endeavors with oral formulations of unmodified peptides such as human insulin and human growth hormone have not advanced beyond preclinical investigations (*32*, *33*).

The absorption-enhancing actions of SNAC are driven by its capacity to mildly perturb the gastric mucosae. Our mechanistic analyses indicate that these effects, including membrane fluidization and surface epithelial sloughing, are transient and fully reversible. Functionally, SNAC administered at different time points before semaglutide was gradually less effective at augmenting permeability, confirming that the duration for enhanced absorption is short (*34*, *35*). Detailed microscopical examinations revealed that the effects are confined to the upper parts of the gastric pits and interfoveolar regions and thus appear entirely superficial. Physiologically, epithelial repair of the gastric mucosa occurs at a rapid rate corresponding to 2 to 5 μm/min, which represents one of the fastest reported migrating cell types (*36*). Mirroring our findings, similar observations are reported after exposure to ethanol or hypertonic sodium chloride solutions (*37*, *38*). The majority (95%) of mucosa exposed to ethanol was repopulated by epithelial cells within 60 min (*36*). Despite its effects on the cell membrane of gastric mucosa, we observed no appreciable effect on tight junction complexes at the apical surface at both light microscopic and ultrastructural degree of detail, which further underscores the transcellular nature of the absorption-enhancing effect of SNAC. Moreover, these observations are consistent with previous reports examining the effects of acetylsalicylic acid and bile salts on gastric mucosa, whereby robust tight junction expression was preserved notwithstanding membrane perturbation (*39*).

In light of the stomach's exposure to semaglutide, we found it prudent to examine GLP-1R localization and amount of expression in the stomach and any functional implications thereof. Using rat and human gastric mucosae, we observed a complete absence of GLP-1R expression in surface mucous epithelial cells, whereas GLP-1Rs were observed in parietal cells and muscle cells of the muscularis externa. Previous reports suggest that GLP-1 has an inhibitory effect on acid secretion (*15*). Measurement of pH in the stomach of humans dosed with oral semaglutide over a period of 10 days revealed no functionally appreciable change. Collectively, these data illustrate that, although semaglutide is transiently present in the stomach lumen at high concentrations, direct engagement with GLP-1Rs does not occur because of its discrete cellular localization distal to the epithelial membrane surface.

Although data presented provide evidence supporting the absorption of semaglutide within the stomach, there remains a dearth of information relating to gastric absorption of drugs and, not least, peptides. Thus, it would be valuable to further examine and discern additional physiological traits of the stomach, which may inform a more complete understanding of (and further rationale for) our observations. Our data emphasize the contiguous interplay between tablet erosion behavior and the establishment of concentration gradients at the absorptive surface, but there remains a need for additional work to appropriately model and compute the kinetics of these processes and the concomitant influence of diffusion, dilution, and spreading on the absorption-enhancing effect of SNAC. Last, although we delineate the route of transepithelial transport harnessed by SNAC as transcellular, further efforts should be applied to particularizing the dynamics of the cellular events dictating the passage of intact semaglutide toward the basolateral membrane and into the systemic circulation.

Here, we describe mechanistic insight into the absorption of an orally administered GLP-1 analog. We reveal the importance of a bespoke approach to combining peptide and absorption enhancer to achieve clinically relevant exposure upon oral administration. Moreover, although we cannot unequivocally exclude some incidental absorption in the intestines, we demonstrate a role for the stomach as a site of absorption for large peptides. The reported findings represent a paradigm shift in our fundamental understanding of peptide absorption after oral administration and a clinically transformative advancement for treatment possibilities for diabetes and/or other chronic diseases by transforming injectable therapies to tablet-based oral medicines.

MATERIALS AND METHODS

Study design

We explored the absorption of oral semaglutide using both clinical and basic science research. The anatomical site of absorption of oral semaglutide was explored in a series of investigations in humans and in various dog models. The interrelationship between semaglutide and SNAC, and particularly, the hypothesis that efficient absorption of oral semaglutide is dependent on the presence of SNAC, was examined in humans, dogs, and in vitro studies. A series of mechanistic animal and in vitro studies were performed to explore how SNAC promotes absorption of oral semaglutide. For the clinical trials, the protocols and the informed consent forms were reviewed and approved by independent ethics committees and appropriate health authorities according to local regulations. The trials were conducted in accordance with the Declaration of Helsinki and the International Conference on Harmonisation Good Clinical Practice. All participants provided written informed consent before any trial-related activities. Sample size determinations in the clinical trials are described in Supplementary Materials and Methods. Participant disposition and baseline characteristics are shown in tables S2 and S3. All animal experiments were carried out in accordance with the Danish Act on Experiments on Animals, the Appendix A of the European Convention for the Protection of Vertebrate Animals used for Experimental and other Scientific Purposes (ETS 123), and European Union Directive 2010/63. The animal numbers generally based on previous experience from pilot studies and power calculations performed to give a statistical power of 80% with a significance level of 5%. Further, paired samples and crossover designs were used whenever possible.

Pharmacoscintigraphic trial

This was a randomized, single-center (Quotient Clinical, Nottingham, UK), open-label, two-period, crossover trial in 26 healthy males, 18 to 64 years with a body mass index (BMI) of 18.5 to 30.0 kg/m^2 (ClinicalTrials.gov identifier: NCT01619345). In one arm of the trial, participants received a single dose of oral semaglutide (10 mg/300 mg of SNAC) administered with 240 ml of water. At each dosing visit, after an overnight fast of ≥8 hours (water ad libitum allowed until 2 hours before dosing), dosing occurred in the morning, followed by ≥4-hour postdose fasting (except for 200 ml of water at 2 hours after dosing). Tablet erosion within the GIT was assessed by gamma scintigraphy using a gamma camera (General Electric Maxicamera, GE Company) with a 40-cm field of view and fitted with a medium-energy parallel-hole collimator. Oral semaglutide tablets contained ^{111}In-labeled ion-exchange resin [≤1 megabecquerel (MBq)]. The water used for tablet administration was labeled with ^{99m}Tc (≤4 MBq; to provide an outline of the GIT). The radiation dose equivalent was ≤0.49 mSv per dosing visit per individual (approved by the Administration of Radioactive Substances Advisory Committee, Oxfordshire, UK). Static dual-isotope (^{111}In and ^{99m}Tc) images of the abdomen were recorded until 4 hours after dosing. Participants were sitting during the first minute. Thereafter, they were standing during the imaging periods but were allowed to sit or remain moderately active in between imaging time points. Blood samples were drawn for analysis of semaglutide (up to 24 hours) and SNAC (up to 6 hours). The scintigraphic data were analyzed using MicasXplus processing software (Bartec Technologies Ltd., Camberley, UK). CTE was defined as the time at which the entire radioactive marker had dispersed into the GIT and no signs of a distinct "core" remained. Semaglutide and SNAC were measured by validated assays using plasma protein precipitation, followed by liquid chromatography–tandem mass spectrometry (LC-MS/MS).

Food-effect trial

This was a randomized, open-label, parallel-group, single-center (Parexel International, Berlin, Germany) trial in 78 healthy individuals, 18 to 75 years with a BMI of 18.5 to 29.9 kg/m^2 (ClinicalTrials.gov identifier: NCT02172313). Participants received once-daily oral semaglutide for 10 days. The oral semaglutide dose was escalated from 5 mg/300 mg of SNAC during the first 5 days to 10 mg/300 mg of SNAC during the last 5 days to mitigate the risk of gastrointestinal adverse events. Participants were randomized into fed, fasting, and reference (not included here) groups (1:1:1). In both fed and fasting groups, participants fasted overnight for ≥10 hours before dosing of oral semaglutide with 240 ml of water. This was followed by a 4-hour postdose fasting period after which a standardized postdose meal [2335 kJ, 49 energy percent (E%) carbohydrate, 34 E% fat, and 17 E% protein) was served. In the fed group, participants consumed a high-calorie, high-fat breakfast (4058 kJ, 27 E% carbohydrate, 60 E% fat, and 13 E% protein) within 30 min before dosing (*40*, *41*). In the fasting group, no predose meal was served. In the trial, the percentage of participants reporting nausea in fed and fasting groups was 0.0 and 30.8%, respectively. Blood samples for analysis of semaglutide were drawn until 504 hours after the 10th dose. Semaglutide was measured by a validated assay using plasma protein precipitation, followed by LC-MS/MS.

First human dose trial

This was a randomized, placebo-controlled, double-blind, single-center (Parexel International, Harrow, UK) trial in 155 healthy males, 18 to 50 years with a BMI of 18.5 to 27.5 kg/m^2 (ClinicalTrials.gov identifier: NCT01037582). The trial consisted of parts 1 and 2 (not included here). In part 1a, four ascending dose groups of oral semaglutide were tested in a sequential design (2, 5, and 10 mg of semaglutide/300 mg of SNAC and 20 mg of semaglutide/600 mg of SNAC). In part 1b, three additional dose groups were tested in a parallel design (5 mg of semaglutide/150 mg of SNAC, 10 mg of semaglutide/600 mg of SNAC, and 15 mg of semaglutide/450 mg of SNAC). In each dose group, 10 and 2 participants were randomized to oral semaglutide and to placebo with SNAC (not included here), respectively. After an overnight fast, participants received a single dose of oral semaglutide or placebo with SNAC administered with 50 ml of water, followed by 5-hour postdose fasting. Blood samples for analysis of semaglutide were drawn until 504 hours after dosing. Semaglutide was measured by a validated luminescence oxygen channeling

immunoassay. It was subsequently found that measurements appeared to be underestimated because of a matrix effect. Therefore, absolute semaglutide concentrations in this trial should be interpreted cautiously, and concentration-time profiles are presented using an arbitrary scale.

Drug-drug interaction trial

This was an open-label, one-sequence, crossover, single-center (Parexel International, Berlin, Germany) trial in 52 healthy individuals, 18 to 75 years with a BMI of 20.0 to 29.9 kg/m^2 (ClinicalTrials.gov identifier: NCT02070510). During a 12-week treatment period, participants received a single dose of 20 mg of lisinopril (Actavis 20 mg, Actavis Nordic) on day 1, a single dose of 25 mg of warfarin (Coumadin 5 mg, Bristol-Myers Squibb) on day 8 (not included here), coadministration of single doses of 20 mg of lisinopril and 300 mg of SNAC on day 15, and coadministration of single doses of 25 mg of warfarin and 300 mg of SNAC on day 22 (not included here). Once-daily oral semaglutide (with 300 mg of SNAC) treatment started on day 29 at a dose of 5 mg for 1 week, 10 mg for 1 week, and 20 mg for 6 weeks. When oral semaglutide was at steady state, participants received coadministration of a single dose of 20 mg of lisinopril on day 71 and a single dose of 25 mg of warfarin on day 78 (not included here). All trial product administrations occurred in the morning after an overnight fast of ≥6 hours and with 30-min postdose fasting. Tablets were administered with 120 ml of water. Blood samples for analysis of lisinopril were drawn until 60 hours after each lisinopril dose. Lisinopril was measured by a validated assay using LC-MS/MS. Pharmacokinetic end points included $AUC_{0-\infty,\text{lisinopril}}$ and $C_{\max,\text{lisinopril}}$.

Gastric pH trial

This was a randomized, open-label, parallel-group, single-center (Parexel, Berlin, Germany) trial in healthy individuals, 18 to 75 years with a BMI of 18.0 to 29.9 kg/m^2 (ClinicalTrials.gov identifier: NCT02249871). Participants received once-daily administration of oral semaglutide (5 mg for 5 days, followed by 10 mg for 5 days) either alone (n = 28) or with concomitant once-daily oral administration of omeprazole (n = 26; not included here). Oral semaglutide tablets were administered in the morning with 120 ml of water after an overnight fast of ≥6 hours and with 30-min postdose fasting. Measurement of gastric pH was performed on the day before first dosing and after 9 days of dosing. A pH catheter was inserted into the stomach via a nostril, and the pH measurements were performed using a ZepHr Impedance/pH reflux monitoring system to record pH every 5 s. The measurement started 2 hours before dosing of oral semaglutide and continued for 5 hours.

Statistical analysis

GraphPad Prism 7 was used for plotting and for statistical analysis of nonclinical data. In Fig. 1F, the 95% CI of the ratio between vena lienalis and vena porta for $AUC_{0-30\text{min}}$ was calculated, and significance was determined on the basis of a null hypothesis value of 1. A two-tailed Student's t test was used to compare 80 mM SNAC versus control in Fig. 2B; to compare $AUC_{0-180\text{min}}$ between semaglutide and liraglutide in Fig. 3A; to compare $AUC_{0-180\text{min}}$ between SNAC and *o*-SNAC in Fig. 3B; to compare SNAC versus control and EDTA versus control in Fig. 3 (D and E); to compare SNAC at a specific time point versus control in Fig. 3H; to compare SNAC versus control and *o*-SNAC versus control in fig. S5; and to compare FD10 (10-kDa fluorescein isothiocyanate–dextran) versus FD4, FD20 versus FD4, and FD150 versus FD4 in fig. S7. In Fig. 2C and fig. S2, statistical analysis was performed using a one-way ANOVA with multiple comparisons. In Fig. 3F, statistical analysis was performed using the Kolmogorov-Smirnov test, comparing TEER values of the control and SNAC-exposed tissue at each time point. In all cases, $P < 0.05$ was considered statistically significant.

Statistical analyses of clinical data were performed using SAS version 9.4 (SAS Institute, Cary, NC, USA). In Fig. 2E, comparisons between coadministration with oral semaglutide or SNAC and lisinopril administration alone were performed using ANOVA models with the log-transformed end point as dependent variable and participant and treatment as fixed effects. No effect of oral semaglutide or SNAC coadministration was concluded if the 90% CI for the ratio of coadministration/alone was within a predefined interval of 0.80 to 1.25. In Fig. 6E, estimates and 95% CIs of 3-hour average pH at baseline and on day 9 were derived and compared using an ANOVA model with logarithmic transformed 3-hour average pH as dependent variable and participant and day (baseline or day 9) as fixed effects. Individual results for data with $n < 20$ are reported in table S4.

SUPPLEMENTARY MATERIALS

www.sciencetranslationalmedicine.org/cgi/content/full/10/467/eaar7047/DC1

Materials and Methods

Fig. S1. Magnetic monitoring of an oral semaglutide tablet in a representative beagle dog.

Fig. S2. Effect of food on semaglutide plasma exposure after oral dosing in beagle dogs.

Fig. S3. Ratio of paracetamol plasma concentrations sampled from splenic/portal veins.

Fig. S4. Arithmetic mean semaglutide plasma concentration–time profiles after a single dose of 10 mg of oral semaglutide with varying amounts of SNAC in healthy males.

Fig. S5. P_{app} of semaglutide across monolayers of NCI-N87 gastric epithelial cells.

Fig. S6. Hemotoxylin and eosin staining of rat gastric mucosa after exposure to buffer alone, SNAC, ethanol, and acetylsalicylic acid.

Fig. S7. Transport of FD4, FD10, FD20, and FD150 across monolayers of NCI-N87 gastric epithelial cells.

Fig. S8. CF leakage assay performed with CF-loaded large unilamellar liposomes composed of DMPC.

Fig. S9. Effect of NaCl on the sedimentation coefficient of semaglutide.

Fig. S10. pH during incubation of semaglutide tablets without SNAC in SGF.

Fig. S11. Enzymatic degradation of native GLP-1 in the presence of pepsin at different pH values.

Fig. S12. Reactivity by 3F15 and 1F46 in the perfusion-fixed rat stomach.

Fig. S13. Mechanism of absorption of oral semaglutide.

Table S1. Bioavailability study of oral semaglutide in beagle dogs.

Table S2. Participant disposition in the clinical trials.

Table S3. Baseline characteristics in the clinical trials.

Table S4. Individual results for data with $n < 20$.

Movie S1. Uptake of semaglutide within blood vessels of the lamina propria mucosae.

Reference (*42*)

REFERENCES AND NOTES

1. J. J. Meier, GLP-1 receptor agonists for individualized treatment of type 2 diabetes mellitus. *Nat. Rev. Endocrinol.* **8**, 728–742 (2012).
2. J. J. Meier, J. Rosenstock, A. Hincelin-Méry, C. Roy-Duval, A. Delfolie, H. V. Coester, B. A. Menge, T. Forst, C. Kapitza, Contrasting effects of lixisenatide and liraglutide on postprandial glycemic control, gastric emptying, and safety parameters in patients with type 2 diabetes on optimized insulin glargine with or without metformin: A randomized, open-label trial. *Diabetes Care* **38**, 1263–1273 (2015).
3. A. Secher, J. Jelsing, A. F. Baquero, J. Hecksher-Sørensen, M. A. Cowley, L. S. Dalbøge, G. Hansen, K. L. Grove, C. Pyke, K. Raun, L. Schäffer, M. Tang-Christensen, S. Verma, B. M. Witgen, N. Vrang, L. Bjerre Knudsen, The arcuate nucleus mediates GLP-1 receptor agonist liraglutide-dependent weight loss. *J. Clin. Invest.* **124**, 4473–4488 (2014).
4. X. Pi-Sunyer, A. Astrup, K. Fujioka, F. Greenway, A. Halpern, M. Krempf, D. C. W. Lau, C. W. le Roux, R. Violante Ortiz, C. B. Jensen, J. P. H. Wilding; SCALE Obesity and Prediabetes NN8022-1839 Study Group, A randomized, controlled trial of 3.0 mg of liraglutide in weight management. *N. Engl. J. Med.* **373**, 11–22 (2015).
5. S. P. Marso, G. H. Daniels, K. Brown-Frandsen, P. Kristensen, J. F. E. Mann, M. A. Nauck, S. E. Nissen, S. Pocock, N. R. Poulter, L. S. Ravn, W. M. Steinberg, M. Stockner, B. Zinman,

R. M. Bergenstal, J. B. Buse; LEADER Steering Committee, LEADER Trial Investigators, Liraglutide and cardiovascular outcomes in type 2 diabetes. *N. Engl. J. Med.* **375**, 311–322 (2016).
6. S. P. Marso, S. C. Bain, A. Consoli, F. G. Eliaschewitz, E. Jódar, L. A. Leiter, I. Lingvay, J. Rosenstock, J. Seufert, M. L. Warren, V. Woo, O. Hansen, A. G. Holst, J. Pettersson, T. Vilsbøll; SUSTAIN-6 Investigators, Semaglutide and cardiovascular outcomes in patients with type 2 diabetes. *N. Engl. J. Med.* **375**, 1834–1844 (2016).
7. J. A. Lovshin, D. J. Drucker, Incretin-based therapies for type 2 diabetes mellitus. *Nat. Rev. Endocrinol.* **5**, 262–269 (2009).
8. J. Lau, P. Bloch, L. Schäffer, I. Pettersson, J. Spetzler, J. Kofoed, K. Madsen, L. B. Knudsen, J. McGuire, D. B. Steensgaard, H. M. Strauss, D. X. Gram, S. M. Knudsen, F. S. Nielsen, P. Thygesen, S. Reedtz-Runge, T. Kruse, Discovery of the once-weekly glucagon-like peptide-1 (GLP-1) analogue semaglutide. *J. Med. Chem.* **58**, 7370–7380 (2015).
9. C. E. Cooke, H. Y. Lee, Y. P. Tong, S. T. Haines, Persistence with injectable antidiabetic agents in members with type 2 diabetes in a commercial managed care organization. *Curr. Med. Res. Opin.* **26**, 231–238 (2010).
10. T. A. Aguirre, D. Teijeiro-Osorio, M. Rosa, I. S. Coulter, M. J. Alonso, D. J. Brayden, Current status of selected oral peptide technologies in advanced preclinical development and in clinical trials. *Adv. Drug Deliv. Rev.* **106**, 223–241 (2016).
11. M. Davies, T. R. Pieber, M.-L. Hartoft-Nielsen, O. K. H. Hansen, S. Jabbour, J. Rosenstock, Effect of oral semaglutide compared with placebo and subcutaneous semaglutide on glycemic control in patients with type 2 diabetes: A randomized clinical trial. *J. Am. Med. Assoc.* **318**, 1460–1470 (2017).
12. M. Tomita, M. Hayashi, S. Awazu, Absorption-enhancing mechanism of EDTA, caprate, and decanoylcarnitine in Caco-2 cells. *J. Pharm. Sci.* **85**, 608–611 (1996).
13. T. M. Frederiksen, P. Sønderby, L. A. Ryberg, P. Harris, J. T. Bukrinski, A. M. Scharff-Poulsen, M. N. Elf-Lind, G. H. Peters, Oligomerization of a glucagon-like peptide 1 analog: Bridging experiment and simulations. *Biophys. J.* **15**, 1202–1213 (2015).
14. D. W. Piper, B. H. Fenton, pH stability and activity curves of pepsin with special reference to their clinical importance. *Gut* **6**, 506–508 (1965).
15. A. Wettergren, M. Wøjdemann, S. Meisner, F. Stadil, J. J. Holst, The inhibitory effect of glucagon-like peptide-1 (GLP-1) 7-36 amide on gastric acid secretion in humans depends on an intact vagal innervation. *Gut* **40**, 597–601 (1997).
16. H. Lennernäs, Regional intestinal drug permeation: Biopharmaceutics and drug development. *Eur. J. Pharm. Sci.* **57**, 333–341 (2014).
17. J. Van Den Abeele, J. Rubbens, J. Brouwers, P. Augustijns, The dynamic gastric environment and its impact on drug and formulation behaviour. *Eur. J. Pharm. Sci.* **96**, 207–231 (2017).
18. S. Maher, R. J. Mrsny, D. J. Brayden, Intestinal permeation enhancers for oral peptide delivery. *Adv. Drug Deliv. Rev.* **106**, 277–319 (2016).
19. M. A. Karsdal, I. Byrjalsen, B. J. Riis, C. Christiansen, Optimizing bioavailability of oral administration of small peptides through pharmacokinetic and pharmacodynamic parameters: The effect of water and timing of meal intake on oral delivery of salmon calcitonin. *BMC Clin. Pharmacol.* **8**, 5 (2008).
20. M. A. Karsdal, I. Byrjalsen, M. Azria, M. Arnold, L. Choi, B. J. Riis, C. Christiansen, Influence of food intake on the bioavailability and efficacy of oral calcitonin. *Br. J. Clin. Pharmacol.* **67**, 413–420 (2009).
21. Y.-H. Lee, B. A. Perry, J. P. Sutyak, W. Stern, P. J. Sinko, Regional differences in intestinal spreading and pH recovery and the impact on salmon calcitonin absorption in dogs. *Pharm. Res.* **17**, 284–290 (2000).
22. J. Worsøe, L. Fynne, T. Gregersen, V. Schlageter, L. A. Christensen, J. F. Dahlerup, N. J. M. Rijkhoff, S. Laurberg, K. Krogh, Gastric transit and small intestinal transit time and motility assessed by a magnet tracking system. *BMC Gastroenterol.* **11**, 145 (2011).
23. K. Whitehead, Z. Shen, S. Mitragotri, Oral delivery of macromolecules using intestinal patches: Applications for insulin delivery. *J. Control. Release* **98**, 37–45 (2004).
24. B. Bittner, C. McIntyre, P. Jordan, J. Schmidt, Drug-drug interaction study between a novel oral ibandronate formulation and metformin. *Arzneimittelforschung* **61**, 707–713 (2011).
25. C. McIntyre, J. Schmidt, M. C. Castelli, B. Bittner, Study on the impact of SNAC (sodium N-[8-(2-hydroxybenzoyl) amino] caprylate) on the bioavailability of ibandronate (IBN) in postmenopausal women. *J. Drug Delivery Sci. Technol.* **21**, 521–525 (2011).
26. J. Wang, V. Yadav, A. L. Smart, S. Tajiri, A. W. Basit, Toward oral delivery of biopharmaceuticals: An assessment of the gastrointestinal stability of 17 peptide drugs. *Mol. Pharm.* **12**, 966–973 (2015).
27. S. H. Welling, F. Hubálek, J. Jacobsen, D. J. Brayden, U. L. Rahbek, S. T. Buckley, The role of citric acid in oral peptide and protein formulations: Relationship between calcium chelation and proteolysis inhibition. *Eur. J. Pharm. Biopharm.* **86**, 544–551 (2014).
28. A. Leone-Bay, D. R. Paton, B. Variano, H. Leipold, T. Rivera, J. Miura-Fraboni, R. A. Baughman, N. Santiago, Acylated non-α-amino acids as novel agents for the oral delivery of heparin sodium, USP. *J. Control Release* **50**, 41–49 (1998).
29. M. Nazari, M. Kurdi, H. Heerklotz, Classifying surfactants with respect to their effect on lipid membrane order. *Biophys. J.* **102**, 498–506 (2012).
30. D. J. Brayden, J. Gleeson, E. G. Walsh, A head-to-head multi-parametric high content analysis of a series of medium chain fatty acid intestinal permeation enhancers in Caco-2 cells. *Eur. J. Pharm. Biopharm.* **88**, 830–839 (2014).
31. S. Trier, L. Linderoth, S. Bjerregaard, T. L. Andresen, U. L. Rahbek, Acylation of glucagon-like peptide-2: Interaction with lipid membranes and in vitro intestinal permeability. *PLOS ONE* **9**, e109939 (2014).
32. D. Malkov, R. Angelo, H.-Z. Wang, E. Flanders, H. Tang, I. Gomez-Orellana, Oral delivery of insulin with the eligen technology: Mechanistic studies. *Curr. Drug Deliv.* **2**, 191–197 (2005).
33. S.-J. Wu, J. R. Robinson, Transcellular and lipophilic complex-enhanced intestinal absorption of human growth hormone. *Pharm. Res.* **16**, 1266–1272 (1999).
34. X. Wang, S. Maher, D. J. Brayden, Restoration of rat colonic epithelium after in situ intestinal instillation of the absorption promoter, sodium caprate. *Ther. Deliv.* **1**, 75–82 (2010).
35. S. Tuvia, D. Pelled, K. Marom, P. Salama, M. Levin-Arama, I. Karmeli, G. H. Idelson, I. Landau, R. Mamluk, A novel suspension formulation enhances intestinal absorption of macromolecules *via* transient and reversible transport mechanisms. *Pharm. Res.* **31**, 2010–2021 (2014).
36. E. R. Lacy, S. Ito, Rapid epithelial restitution of the rat gastric mucosa after ethanol injury. *Lab. Invest.* **51**, 573–583 (1984).
37. S. Ito, E. R. Lacy, M. J. Rutten, J. Critchlow, W. Silen, Rapid repair of injured gastric mucosa. *Scand. J. Gastroenterol. Suppl.* **101**, 87–95 (1984).
38. E. R. Lacy, G. P. Morris, M. M. Cohen, Rapid repair of the surface epithelium in human gastric mucosa after acute superficial injury. *J. Clin. Gastroenterol.* **17**, S125–S135 (1993).
39. G. L. Eastwood, Effect of pH on bile salt injury to mouse gastric mucosa. A light- and electron-microscopic study. *Gastroenterology* **68**, 1456–1465 (1975).
40. U.S. Food and Drug Administration, Guidance for industry: Food-effect bioavailability and fed bioequivalence studies, December 2002. www.fda.gov/downloads/drugs/guidancecomplianceregulatoryinformation/guidances/ucm070241.pdf.
41. European Medicines Agency, Committee for human medicinal products: Guideline on the investigation of drug interactions, 21 June 2012. www.ema.europa.eu/docs/en_GB/document_library/Scientific_guideline/2012/07/WC500129606.pdf.
42. W. Weitschies, H. Blume, H. Mönnikes, Magnetic marker monitoring: High resolution real-time tracking of oral solid dosage forms in the gastrointestinal tract. *Eur. J. Pharm. Biopharm.* **74**, 93–101 (2010).

Acknowledgments: We thank C. Roepstorff (CR Pharma Consult, Copenhagen, Denmark) for providing medical writing support and Spirit Medical Communications (Manchester, UK) for providing scientific illustration support, which was funded by Novo Nordisk A/S. **Funding:** This work was supported by Novo Nordisk A/S. **Author contributions:** S.T.B., T.A.B., A.V., C.P., and L.B.K. conceived and designed the research. T.A.B., S.J.M., J.B., and M.-L.H.-N. coordinated clinical investigations. A.V., R.B.S., and R.K.K. performed in vivo animal studies. S.T.B., S.G.S., K.G.M., B.L.P., and S.B. performed the in vitro characterization. A.J.B., H.M.S., and P.-O.W. performed the biophysical characterization. C.P., J.A.-R., T.A., and R.K.K. performed histology and imaging studies. E.F. and C.F. performed EM studies. F.L.S. performed the statistical analysis on clinical data. S.T.B., T.A.B., A.V., S.J.M., C.P., and L.B.K. analyzed data and wrote the manuscript. **Competing interests:** S.T.B., T.A.B., A.V., S.J.M., C.P., J.A.-R., K.G.M., S.G.S., R.K.K., R.B.S., H.M.S., S.B., F.L.S., M.-L.H.-N., and L.B.K. are shareholders of Novo Nordisk A/S. S.T.B., T.A.B., A.V., C.P., J.A.-R., K.G.M., R.K.K., R.B.S., A.J.B., P.-O.W., F.L.S., J.B., M.-L.H.-N., and L.B.K. are current employees of Novo Nordisk A/S., S.J.M., S.G.S., T.A., B.L.P., H.M.S., and S.B. were employees of Novo Nordisk A/S at the time of conducting the studies. C.F. has received funding from Novo Nordisk A/S. E.F. declares no competing interest. **Data and materials availability:** All data associated with this study are present in the paper or the Supplementary Materials. Data and reagents may be made available upon reasonable request from Novo Nordisk A/S under a materials transfer agreement.

Submitted 21 February 2018
Accepted 22 October 2018
Published 14 November 2018
10.1126/scitranslmed.aar7047

Citation: S. T. Buckley, T. A. Bækdal, A. Vegge, S. J. Maarbjerg, C. Pyke, J. Ahnfelt-Rønne, K. G. Madsen, S. G. Schéele, T. Alanentalo, R. K. Kirk, B. L. Pedersen, R. B. Skyggebjerg, A. J. Benie, H. M. Strauss, P.-O. Wahlund, S. Bjerregaard, E. Farkas, C. Fekete, F. L. Søndergaard, J. Borregaard, M.-L. Hartoft-Nielsen, L. B. Knudsen, Transcellular stomach absorption of a derivatized glucagon-like peptide-1 receptor agonist. *Sci. Transl. Med.* **10**, eaar7047 (2018).

Science Translational Medicine

Transcellular stomach absorption of a derivatized glucagon-like peptide-1 receptor agonist

Stephen T. Buckley, Tine A. Bækdal, Andreas Vegge, Stine J. Maarbjerg, Charles Pyke, Jonas Ahnfelt-Rønne, Kim G. Madsen, Susanne G. Schéele, Tomas Alanentalo, Rikke K. Kirk, Betty L. Pedersen, Rikke B. Skyggebjerg, Andrew J. Benie, Holger M. Strauss, Per-Olof Wahlund, Simon Bjerregaard, Erzsébet Farkas, Csaba Fekete, Flemming L. Søndergaard, Jeanett Borregaard, Marie-Louise Hartoft-Nielsen and Lotte Bjerre Knudsen

Sci Transl Med **10**, eaar7047.
DOI: 10.1126/scitranslmed.aar7047

Assisting absorption

Glucagon-like peptide-1 receptor agonists can help treat type 2 diabetes but must be administered by injection. Toward developing an effective oral therapy, Buckley *et al*. tested whether coformulating an oral GLP-1 analog, semaglutide, with SNAC, a small fatty acid derivative, improved drug absorption. Unlike most drugs, the coformulation was absorbed in the stomach rather than in the intestine. In animal studies and human trials, SNAC buffered the local pH of the stomach to protect against enzymatic degradation and facilitate transepithelial absorption via the transcellular route. These results suggest that the transient absorption enhancement offered by SNAC coformulation may help develop effective oral peptide–based therapies.